Published in final edited form as:
Ultrasound Med Biol. 2014 February ; 40(2): 341–350. doi:10.1016/j.ultrasmedbio.2013.09.016.

Ex Vivo Characterization of Canine Liver Tissue Viscoelasticity Following High Intensity Focused Ultrasound (HIFU) Ablation

Danial Shahmirzadi[1], **Gary Y. Hou**[1], **Jiangang Chen**[1], and **Elisa E. Konofagou**[1,2]

[1]Ultrasound and Elasticity Imaging Laboratory, Department of Biomedical Engineering

[2]Department of Radiology, Columbia University, New York, NY 10032

Abstract

Elasticity imaging has shown great promise in detecting High Intensity Focused Ultrasound (HIFU) lesions based on their distinct biomechanical properties. However, quantitative mechanical properties of the tissue and the optimal intensity for obtaining the best contrast parameters remain scarce. In this study, fresh canine livers were ablated using combinations of I_{SPTA} intensities of 5.55, 7.16 and 9.07 kW/cm^2 and time durations of 10 and 30 *s ex vivo*; leading to six groups of ablated tissues. Biopsy samples were then interrogated using dynamic shear mechanical testing within the range of 0.1-10 *Hz* to characterize the post-ablation tissue viscoelastic properties. All mechanical parameters were found to be frequency dependent. Compared to the unablated cases, all six groups of ablated tissues showed statistically-significant higher complex shear modulus and shear viscosity. However, among the ablated groups, both complex shear modulus and shear viscosity were found to monotonically increase in groups 1-4 (5.55 kW/cm^2 for 10 *s*, 7.16 kW/cm^2 for 10 *s*, 9.07 kW/cm^2 & 10 *s*, and 5.55 kW/cm^2 & 30 *s*, respectively), but decrease in groups 5 and 6 (7.16 kW/cm^2 for 30 *s*, and 9.07 kW/cm^2 for 30 *s*, respectively). For groups 5 and 6, the temperature was expected to exceed the boiling point, and therefore, the decreased stiffening could be due to the compromised integrity of the tissue microstructure. Future studies are needed to estimate the tissue mechanical properties *in vivo* and perform real-time monitoring of tissue alterations during ablation.

Keywords

Canine liver; Elasticity Imaging; HIFU; HMIFU; Thermal ablation; Viscoelasticity

Corresponding author: Elisa E. Konofagou, Department of Biomedical Engineering, Columbia University, 1210 Amsterdam Ave, ET 351, MC 8904, New York, NY 10027, ek2191@columbia.edu, Tel: 212.342.0863, Fax: 212342.1648.

Conflict of Interests- There are no conflicts of interest in this study to disclose.

Introduction

The mechanical properties of soft tissues have been shown to change under pathological conditions (Anderson 1957; Krouskop et al. 1998; Blacher et al. 2001; Marra et al. 2006; Weinberg et al. 2010; Shahmirzadi and Konofagou 2012). In particular, liver stiffness has been shown to change during various liver pathologies and has been used as a diagnosis marker (Mueller and Sandrin 2010; Godfrey et al. 2013; Venkatesh et al. 2013).

Elasticity imaging denotes the field of mapping tissue mechanical response *in situ* under either external perturbation such as static elastography (Ophir et al. 1991), dynamic elastography (Parker et al. 1990; Shi et al. 1999), and Magnetic Resonance Elastography (MRE) (Muthupillai et al. 1995; Kruse et al. 2000; Godfrey et al. 2013); or internal perturbation such as vibroacoustography (Fatemi and Greenleaf 1998), shear wave imaging (Sarvazyan et al. 1998; Bercoff et al. 2004; Sapin de Brosses et al. 2010; Sapin de Brosses et al. 2011; Wang et al. 2012; Frulio and Trillaud 2013), and Acoustic Radiation Force Impulse (ARFI) elasticity imaging (Nightingale et al. 2001). Studies have shown the feasibility of using elasticity imaging techniques to quantify elastic properties of various soft tissues (Meunier et al. 1988; Cespedes et al. 1993; Emelianov et al. 1995; Kallel et al. 1999a; Bercoff et al. 2003; Alizad et al. 2005; Zhang et al. 2008; Couade and al. 2010; Damianou et al. 2010; Granke et al. 2011; Shahmirzadi et al. 2012; Wang et al. 2012). Particularly, different elasticity imaging techniques have been used for measuring mechanical properties of liver in healthy and pathological condition, aiming to improve the non-invasive diagnosis of liver diseases (Frizzell et al. 1977; Ter Haar et al. 1991a; Sandrin et al. 2003; Antolin et al. 2009; Damianou et al. 2010; Frulio and Trillaud 2013).

High-Intensity Focused Ultrasound (HIFU) has shown over the past decade to be a potentially promising non-invasive therapeutic method (Vallancien et al. 1992; Wu et al. 1999; Li et al. 2004; Wu et al. 2005a; Wu et al. 2005b). An emerging application for ultrasound–based elasticity imaging techniques has been the assessment and monitoring of change in tissue mechanical properties during HIFU procedure (Fry et al. 1954; Basauri and Lele 1962; Warwick and Pond 1968; Kallel et al. 1999b; Righetti et al. 1999; Wu et al. 2001; Souchon et al. 2005; Chenot et al. 2010; Arnal et al. 2011; Thittai et al. 2011). Harmonic Motion Imaging for Focused Ultrasound (HMIFU) is a radiation-force-based HIFU treatment monitoring technique with feasibility shown *in silico*, *in vitro*, *ex vivo*, and *in vivo* (Maleke et al. 2005; Maleke and Konofagou 2008; Maleke and Konofagou 2009; Hou et al. 2010; Hou et al. 2011; Hou et al. 2012a; Hou et al. 2012b). In HMIFU, a focused transducer is used to induce focal ablation while a confocal pulse-echo transducer is simultaneously used to image the tissue and estimate the Harmonic Motion Imaging (HMI) displacements and phase shift, which aim to monitor and assess the lesion-to-medium contrast. Preliminary studies have been carried out to estimate the mechanical properties of materials using numerical and phantom HMI studies (Vappou et al. 2009; Vappou et al. 2013). In order to further enhance the HMI monitoring and assessment capabilities, independent characterization of the change in the tissue viscoelastic properties under HIFU ablation is warranted. Soft tissue mechanical properties have been found to usually undergo a (reversible) softening under increasing temperature, followed by a (irreversible) stiffening beyond certain temperatures (Wu et al. 2001; Maleke and Konofagou 2008; Sapin de

Brosses et al. 2010). Few studies have also compared the results of elasticity imaging of HIFU-induced thermal lesions to those from conventional mechanical testing and have reported a lesion stiffness contrast ranging between four to twelve times compared to unablated tissue (Righetti et al. 1999; Shi et al. 1999; Wu et al. 2001; Hou et al. 2011). Nevertheless, a very limited amount of literature exists on the tissue mechanical properties under high ablation powers.

Obtaining the viscoelastic properties of the ablated tissues has been suggested to provide more comprehensive measures and to carry more potential for efficient treatment monitoring. Dynamic elastometry has been used to obtain the elastic properties of porcine liver tissue under HIFU ablation and resulted in 26 % underestimation of the Young's modulus as measured by mechanical testing (Shi et al. 1999). More recently, the results of transient elastography in characterizing the porcine liver shear modulus *in vivo* have been found to be in good agreement with those of dynamic shear testing *ex vivo* (Chatelin et al. 2011). Gao *et al.* have performed shear, compression and tensile mechanical testing on porcine livers *ex vivo* and used the experimental data to develop energy-based constitutive models of liver tissue (Gao et al. 2010). An advanced shear rheometry instrument has been used to measure the shear and loss moduli of bovine liver *ex vivo* under a high frequency range of 25-62.5 *Hz*, and have been compared against those obtained on human liver using MRE *in vivo* (Klatt et al. 2010). Brunon *et al.* has tested the failure of porcine and post-mortem human livers using tensile testing *ex vivo* (Brunon et al. 2010). Kiss *et. al.* used compressive Dynamic Mechanical Analysis (DMA) of canine and porcine liver tissues and showed that both the magnitude and phase shift of the tissue complex modulus rose monotonically as the loading frequency increases (Kiss et al. 2009). The same study has shown that the magnitude and phase shift of the complex modulus also increase with temperature up to around 75°*C* and decreases afterward up to the reported temperature of 90°*C*; explained likely due to gelation of collagen (Kiss et al. 2009).

In the present study, we investigated the effects of HIFU ablation on the viscoelastic properties of freshly excised canine liver specimens. Given the stochastic nature of boiling effects on tissue properties, we expect that the mechanical and structural changes in ablated liver tissues are different within the ranges of intensities and time periods used in this study. Having quantified knowledge of such changes can be helpful in targeting different levels of ablation that best fits the purpose of the HIFU application.

Materials and Methods

Sample Preparation

Six canine liver specimens were freshly excised immediately after sacrifice and kept immersed in degassed PBS throughout the experiments *ex vivo*. The experiments on each liver were completed within 2-3 hours post-mortem. All procedures were approved by the Institutional Animal Care and Use Committee (IACUC) at Columbia University.

HIFU Ablation

Figure 1 illustrates the schematics of the HIFU experimental set up. The samples were placed over an acoustic absorber submerged in degassed PBS bath. A customized Focused Ultrasound (FUS) system (*Riverside Research Institute, NY*) was used in this study to induce HIFU lesions in the liver samples. The HIFU transducer was a custom made PZT probe with center frequency at 4.755 *MHz*. The focusing depth was 9.5 *cm* and the focal spot size on the -6 *dB* transmit beam was 5×0.4 mm^2. The transducer was driven by an amplitude-modulated CW waveform sequence generated by a set of two function generators (Agilent 33120A & 33220A). The first one produces a carrier frequency of 4.755 *MHz*, and the second one modulates the first externally to produce a signal modulation frequency of 25 *Hz* (leading to a frequency of 50 *Hz* on intensity/force waveform). The amplitude modulation was necessary in order to induce the oscillatory motion within the frequency range that allows the tissue to enter steady-state oscillations that can be measured by HMI. In order to provide a sufficiently large and homogenously ablated region for subsequent extraction of mechanical testing samples, a raster scan was performed on a grid of 7×7 to 9×9 points in order to generate a conglomerate set of thermal lesions spanning across an area varying between 1.5×1.5 cm^2 and 2.5×2.5 cm^2, respectively, depending on the various ablation power intensities and time periods. The raster scan was performed using a MATLAB-programmed, 3-D translational positioning system (*Velmex Inc., Lachine, QC, Canada*). The entire assembly of HIFU and imaging transducers was being moved together during the raster scan. The confocally-aligned, 7.5-*MHz* pulse-echo imaging transducer (*V320-SU-PTF, Olympus NDT, MA*) was used to acquire RF signals for displacement estimation with HMI. A portion of each liver was examined unablated as the control group, group 0, and the rest were ablated under different ablation intensities and time durations, forming ablated groups 1-6. A summary of ablation parameters in each group is provided in Table 1. In situ intensity I_{SPTA} was extrapolated based on hydrophone measurements in the water tank on the same transducer at a lower intensity range; with consideration of canine liver tissue attenuation of -0.75 *dB/cm* (Hou et al. 2011).

Rheometry Mechanical Testing

After completion of the ablation, both unablated and ablated tissues were sectioned for mechanical testing using shear rheometry *(ARES-G2, TA Instrument, DE, USA)*. A 6 *mm* biopsy punch was used to extract a total of forty-four (n=44) cylindrical samples of height h=4.68±0.39 *mm* and diameter d=5.69±0.37 *mm* from the unablated tissues in group 0 (n=13) as well as ablated tissues in group 1 (n=4), group 2 (n=4), group 3 (n=7), group 4 (n=8), group 5 (n=8) and group 6 (n=8). First, a 5% compressional strain was applied on the samples to increase the shear surface grip between the tissue-fixture interfaces. The oscillatory shear test was performed by applying a periodic shear strain, $\gamma(t)$, as follows:

$$\gamma(t)=\gamma_0\sin(\omega t)=\gamma_0\sin(2\pi f t), \quad (1)$$

where γ_0 is the magnitude of the shear strain, t is time, and ω and f are the radial and linear frequency, respectively; and measuring the resultant shear stress, $\tau(t)$, in the form of:

$$\tau(t)=\tau_0\sin(\omega t+\delta)=\tau_0\sin(2\pi f t+\delta). \quad (2)$$

where τ_0 is the magnitude of the shear stress and δ is the phase shift between stress and strain. The applied shear strain was set at $\gamma_0 = 0.01$ within a sweeping frequency range of $f = 0.1 – 10$ *Hz*. The strain and stress magnitudes were used to calculate the complex shear modulus, G^*, as follows:

$$G^* = \tau_0 / \gamma_0. \quad (3)$$

The complex shear modulus and phase shift were also used to compute the shear loss (viscous) modulus, G'', and storage (elastic) modulus, G', as follows, respectively:

$$G'' = G^*\sin\delta = \tau_0 / \gamma_0 \sin\delta, \quad (4)$$

$$G' = G^*\cos\delta = \tau_0 / \gamma_0 \cos\delta. \quad (5)$$

Additionally, the ratio of the viscosity to elasticity as represented by $\tan\delta$, and the dynamic shear viscosity coefficient, η'', were calculated as follows, respectively:

$$\tan\delta = G'' / G', \quad (6)$$

$$\eta'' = G'' / \omega = \tau_0 / \gamma_0\omega \sin\delta. \quad (7)$$

Statistical Significance

All 8 animals used in the study were from the same breed, age/weight range and diet, and therefore were safely assumed to be from the same population. A Student's (unpaired) t-test analysis was performed to obtain the significance of inter-group difference in the experimental data. Given the HMI frequency of 50 *Hz*, the mechanical measurements at 10 *Hz* were found to be the most relevant and were considered for statistical analysis. The significance was computed both between the unablated group and each of the ablated groups, *i.e.* groups 0&1, 0&2, … 0&5 and 0&6, as well as between each of the consecutive ablated groups, *i.e.* groups 1&2, 2&3, …, 4&5 and 5&6. Inter-group difference with significance $p<0.05$ and $p<0.001$ are marked with * and **, respectively.

Results

Figure 2 shows an example of a gross pathology image of a conglomerate group of lesions forming a large inclusion inside a liver specimen using raster HIFU ablation. Figures 3-5 indicate the rheometry measurements on shear complex modulus, G^*, tangent of the phase

shift, $tan\delta$, and the viscosity coefficient, η'', respectively, for the unablated tissue, group 0, and the ablated tissues, groups 1-6, as a function of shear strain frequency, *f* (logarithmic scale). All three parameters were found to be frequency–dependent; a direct relationship for the shear modulus, similar to the data reported elsewhere (Kiss et al. 2009), and an inverse relationship for the shear viscosity coefficient. Table 2 summarizes the relative changes in the mechanical parameters of the ablated tissues, normalized to the unablated tissue, averaged over the entire frequency range.

Shear complex modulus for all ablated tissues was found approximately an order of magnitude higher than that of the unablated tissue, group 0, *i.e.* average of 5.77, 9.83, 19.98, 23.09, 13.66 and 14.06 times for groups 1-6, respectively (Table 2); showing higher stiffening in ablated samples in groups 1-4. The measurements from all ablated groups were found to be statistically different from those from unablated group; however, between the ablated groups, only groups 2 and 3 showed significant difference (Fig. 3). The tangent of the phase shift in all ablated tissues was significantly higher than those in the unablated cases. In contrast, the changes in the same variable were insignificant among the ablated groups (Fig. 4). Similar to shear complex modulus, the dynamic shear viscosity coefficient of ablated tissues was also found significantly higher than that of the unablated group (Fig. 5), *i.e.* average of 8.19, 12.98, 25.49, 30.14, 16.95 and 19.02 times for groups 1-6, respectively (Table 2).

In order to compare the relative contributions of tissue viscosity and elasticity components to the overall tissue viscoelastic behavior, the shear loss (viscous) modulus and storage (elastic) modulus of the unablated and all ablated tissues are plotted against each other along the frequency as the azimuth axis (Fig. 6-A); with its projection on the storage–loss moduli plane shown in Fig. 6-B. The dashed line in the Fig. 6-B indicates the border on which the loss and storage moduli are equal. The overall viscoelastic behavior of both the unablated and all ablated tissues is dominated by the elastic component rather than the viscous component.

The mechanical testing measurements at 10 *Hz* are on the same order of magnitude as the typical HMI application at 50 *Hz*. Figure 7 shows the change in the shear modulus, tangent of the phase shift and shear viscosity of the tissue samples at 10 *Hz* only. The results show that the changes in the parameters are different depending on the range of intensity and time. For instance, under the lower intensities of 5.55 and 7.16 kW/cm^2, the shear modulus increases with duration from 10 to 30 *s*; however, at the higher intensity of 9.07 kW/cm^2, the shear modulus decreases with duration from 10 to 30 *s* (Fig. 7-A). Interpreting the same data with treatment duration as an independent variable, it was found that for shorter ablation duration of 10 *s*, the shear modulus increases with intensities of 5.55, 7.16 and 9.07 kW/cm^2; however, at the longer duration of 30 *s*, the modulus decreases with intensity (Fig. 7-A).

Discussion

The changes in the tissue mechanical properties during pathological conditions have been the basis for various diagnostic techniques. Recent improvements in elastography have made it a promising technique for noninvasive estimation of the tissue focal mechanical properties

in situ. Using very high HIFU intensities over long periods of time has shown to be potentially relevant in ablating the tumorous lesions in the tissues in order to achieve a full tumor treatment (Ter Haar et al. 1991b). Due to variations in structural and mechanical changes in soft tissues with temperature, the possibility of thermal necrosis by heating, and tissue emulsification by cavitation or by use of repetitive millisecond shock wave-based boiling have all been recently discussed (Khokhlova et al. 2011). Within a low temperature range, *i.e.* 42-46 °*C*, only apoptosis has been shown to occur (Badini et al. 2003), however, much higher temperature increase have shown to replace natural apoptosis by forced necrosis where severely damaged cells permeate into the tissue extracellular matrix (Samali et al. 1999; Kiss et al. 2009). Shear elasticity imaging of porcine liver during histotripsy ex vivo has shown the Young's modulus to linearly correlate with the number of structurally-intact cell nuclei (Wang et al. 2012). In order to further enhance the monitoring and assessment capabilities of the elasticity imaging-based techniques, independent estimations of the change in tissue viscoelastic properties are very helpful. The mechanical properties of ablated lesions, particularly under high energies, have remained largely understudied.

This study aims at characterizing the effects of HIFU ablation intensity and time period on the viscoelastic properties of the canine liver tissues. Shear rheometry measurements were made on tissues ablated under HIFU intensities of 5.55, 7.16 and 9.07 kW/cm^2, over time periods of 10 and 30 *s*. An average complex shear modulus of about 3 *kPa* was measured in unablated liver tissues –consistent with measurements reported elsewhere (Kruse et al. 2000; Kiss et al. 2009).

Shear complex modulus for ablated tissues in groups 1-6 was found to be 5.77, 9.83, 19.98, 23.09, 13.66 and 14.06 times higher than the unablated tissues, group 0, respectively (Table 2), which shows that a monotonic increase in ablation intensity and/or time period does not correspond to a monotonic increase in the tissue modulus. A similar trend has previously been reported in porcine liver tissue ablated using boiling (Kiss et al. 2009). That study indicated an increase of up to 6-11 times in the complex modulus as the temperature rises from 40 °*C* to about 75 °*C*, beyond which it decreased about 10-20 % up to the tested temperature of about 90 °*C*. A similar trend was also found for the change in viscosity coefficients of the ablated tissues as a function of HIFU intensity and time; groups 1-6 were found to have viscosities to be 8.19, 12.98, 25.49, 30.14, 16.95 and 19.02 times higher than thaoe of unablated tissues, respectively (Table 2). These findings could be explained based on the fact that unlike in thermal ablation at lower energies, which causes cell shrinkage and stiffening of thermally–coagulated tissue (Wiederhorn and Reardon 1952; McGee 1984), increasing ablation energies may induce tissue emulsification, as a result of which the tissue strength is reduced due to compromised structural integrity of gelated collagen (Kiss et al. 2009).

An alternative parameter to ablation energy or power in controlling tissue damage is to estimate the thermal dose applied during the ablation (Sapin de Brosses et al. 2011). Due to the limitation in the current experimental set up in making temperature measurements during HIFU, thermal dose could not be obtained. Inserting thermocouple at the focal zone inside the tissue induces artifacts in our study, mostly because of large absorption, which requires generation of homogenous ablated legion. However, using a T-type bare wire thermocouple

with diameter of 25 *μm* (*Omega Inc., Stamford, CT*) described in more details elsewhere (Wang et al. 2011), our findings from another study on temperature monitoring on the same canine liver tissue under same range of HIFU intensities and time periods have confirmed the temperature in group 4 reaching the boiling point (Hou et al. 2013). No measurements were able to be made in groups 5 and 6 –due to the thermocouple limitation in measuring temperatures beyond boiling; however, strong damage to tissue microstructure is expected to take place.

All viscoelastic behaviors were found to be frequency dependent: direct relationship for shear modulus, and inverse relationship for viscosity coefficient (Figs. 3-6). Applying shear strain under frequencies higher than 10 *Hz* was not possible due to mechanical limitations of the rheometry system. Given the range of HMI frequency to be higher, e.g. 50 *Hz* (Hou et al. 2011; Hou et al. 2013) than what is examined in the rheometry testing here, the mechanical measurements made at 10 *Hz*, i.e. closest to the HMI frequency, were particularly used in obtaining the contrast plots (Fig. 7). The tangent of the phase shift was the least sensitive parameter for monitoring the change in tissue properties under ablation (Fig. 7-B), whereas the shear modulus and viscosity may found to be more relevant parameters for such purposes (Figs. 7-A & 7-C). More importantly, the results in Fig. 7 indicated that the changes in mechanical properties of the ablated tissues depend on both intensity and time period of the HIFU application. For example, Fig. 7-A showed that under the lower intensities of 5.55 and 7.16 kW/cm^2, the shear modulus increased for longer time periods of 30 s, compared to 10 s. However, at the higher intensity of 9.07 kW/cm^2, decrease in the shear modulus was found by increasing the ablation time period from 10 to 30 *s*. Alternatively, the shear modulus was found to increase with intensity in the shortest ablation duration case. However, for the longer treatment duration of 30 *s*, the shear modulus was found to decrease with intensity.

The HMIFU has been demonstrated by our group to be capable of detecting lesions based on the lesion-to-background displacement contrast (Hou et al. 2012a; Hou et al. 2013). However, the comparison of the modulus contrast between the present study and the HMIFU study requires obtaining the focal radiation force as it could vary given the change in tissue acoustic properties, such as attenuation, as a function of depth and temperature (Gertner et al. 1997; Techavipoo et al. 2002). In particular, focal increase in lesion attenuation can occur (Shi et al. 1999) because of boiling and thermal effects, resulting in an increase in radiation force and induced displacement (Hou et al. 2013). The dominant factor of attenuation in soft tissues is known to be absorption, and therefore the HMI displacements here are primarily generated by the acoustic radiation force, corresponding to the absorption of HIFU energy at the focal spot.

The relatively large standard deviations in the liver tissue property measurements could be associated with the large variations inherent to the liver tissues, particularly under strong thermal effects which have been previously shown to induce changes of highly stochastic and locally– variant nature (Xu et al. 2007; Khokhlova et al. 2011). Also, the inhomogeneity of the lesions obtained by raster HIFU ablation has been shown to contribute to the variations in the ablated tissue properties (Zhou 2013). Here, initial studies were carried out to identify the suitable lesion size and location for each ablation intensity and time.

Furthermore, the mechanical properties of the liver tissue have been shown to contribute to the change during heating and cooling *ex vivo*, e.g. liver tissue stiffens during cooling (Sapin de Brosses et al. 2010). Given the metabolic nature of liver tissues, it is expected that the mechanical and structural properties of the samples postmortem not only varied across the tissue samples, but was also different from the liver tissue *in vivo*. Nevertheless, *ex vivo* findings on mechanical and structural properties of liver under healthy and pathological conditions have widely been used to better understand the disease mechanisms and *in vivo* findings (Brunon et al. 2010; Gao et al. 2010; Klatt et al. 2010; Chatelin et al. 2011; Huang et al. 2011; DeWall et al. 2012). The primary objective of this study was to obtain the tissue mechanical property contrast between the lesion and the background. Therefore, the *ex vivo* testing was indeed found helpful in increasing the repeatability of the mechanical testing measurements by making the entire raster ablated lesion more thermally and mechanically homogeneous. Inherent to the mechanical testing is the fact that the measurements are highly dependent on factors such as sample size, shape and the boundary conditions (Chen et al. 1996; Kallel et al. 1998; Shi et al. 1999). To minimize such confounding effects, all specimens undergoing mechanical testing were prepared with the same shape and size and were extracted from homogenously ablated regions of the lesion.

Conclusion

Independent estimation of mechanical properties of HIFU soft tissue lesions is warranted for enhancement of the monitoring and treatment procedures. Currently, real-time measurements of tissue modulus *in situ* during HIFU ablation might not be readily possible. As an alternative, the present work described the characterization of viscoelastic properties of canine liver tissues *ex vivo* following HIFU ablation under intensities of 5.55, 7.16 and 9.07 kW/cm^2 and time periods of 10 and 30 *s*. The results showed an order of magnitude increase in the stiffness (*e.g.* 6-23 times) and viscosity (*e.g.* 8-30 times) of all ablated lesions. However, monotonic increase in ablation intensity and time period was found not to correspond to monotonic increase in the lesion modulus and viscosity. The mechanical properties were also found to be frequency-dependent within the interrogated range of 0.1-10 *Hz*. Furthermore, the contrast plots of the mechanical properties at 10 *Hz* –closest to the typical HMI frequency 50 *Hz*– were provided and showed that the change in mechanical parameters depends on both the ablation intensity and time. The findings in this study led to the hypothesis that a multi-parametric assessment of frequency-dependent tissue properties may prove more efficient in assessing tissue ablation, and potentially useful in future improvements of the treatment monitoring.

Acknowledgments

This project was supported by the National Institutes of Health (R01EB014496 & R21EB008512). We would like to thank the HMI group members from our lab, Drs. F. Marquet, S. Nandlall and S. Wang for helping with the experimental design and having helpful discussions throughout the study. We would also like to extend our gratitude to Prof. P. A. Boyden and W. Dun at the Center for Molecular Therapeutics of Columbia University for providing us with the animal specimens; and Prof. V. C. Mow, director of the Functional Tissue Engineering Research Lab, and Dr. Leo Q. Wan from the department of biomedical engineering at Columbia University for providing the mechanical testing systems. We also thank the Riverside Research Institute, New York, for providing the therapeutic transducer and helping with the application design.

References

Alizad A, Whaley DH, Greenleaf JF, Fatemi M. Potential applications of vibro-acoustography in breast imaging. Technol Cancer Res T. 2005; 4:151–7.

Anderson, WAD. Pathology. St. Louis: The C. V. Mosby Company; 1957.

Antolin GS, Pajares FG, Vallecillo MA, Orcajo PF, de la Cuesta SG, Alcaide N, Sagrado MG, Velicia R, Caro-Paton A. FibroScan Evaluation of Liver Fibrosis in Liver Transplantation. Transpl P. 2009; 41:1044–6.

Arnal B, Pernot M, Tanter M. Monitoring of Thermal Therapy Based on Shear Modulus Changes: II. Shear Wave Lesion Imaging of Thermal Lesions. IEEE Trans Ultrason Ferroelectr Freq Control. 2011; 58:1603–11. [PubMed: 21859579]

Badini P, de Cupis P, Gerosa G. Necrosis evolution during high- temperature hyperthermia through implanted heat sources. IEEE Trans Biomed Eng. 2003; 50:305–15. [PubMed: 12669987]

Basauri L, Lele PP. A simple method for production of trackless focal lesions with focused ultrasound: statistical evaluation of the effects of irradiation on the central nervous system of the cat. J Physiol. 1962; 160:513–34. [PubMed: 16992120]

Bercoff J, Chaffai S, Tanter M, Sandrin L, Catheline S, Fink M, Gennisson JL, Meunier M. In vivo breast tumor detection using transient elastography. Ultrasound in Medicine and Biology. 2003; 29:1387–96. [PubMed: 14597335]

Bercoff J, Tanter M, Fink M. Supersonic shear imaging: A new technique for soft tissue elasticity mapping. Ieee T Ultrason Ferr. 2004; 51:396–409.

Blacher J, Guerin AP, Pannier B, Marchais SJ, London GM. Arterial calcifications, arterial stiffness, and cardiovascular risk in end-stage renal disease. Hypertension. 2001; 38:938–42. [PubMed: 11641313]

Brunon A, Bruyere-Garnier K, Coret M. Mechanical characterization of liver capsule through uniaxial quasi-static tensile tests until failure. J Biomech. 2010; 43:2221–7. [PubMed: 20394930]

Cespedes I, Ophir J, Ponnekanti H, Maklad N. Elastography - Elasticity Imaging Using Ultrasound with Application to Muscle and Breast in-Vivo. Ultrasonic Imaging. 1993; 15:73–88. [PubMed: 8346612]

Chatelin S, Oudry J, Périchon N, Sandrin L, Allemann P, Soler L, Willinger R. In vivo liver tissue mechanical properties by transient elastography: Comparison with dynamic mechanical analysis. Biorheology. 2011; 48:75–88. [PubMed: 21811013]

Chen EJ, Novakofski J, Jenkins WK, O'Brien WD. Young's Modulus Measurements of Soft Tissues with Application to Elasticity Imaging. IEEE Trans Ultrason Ferroelectr Freq Control. 1996; 43:191–4.

Chenot J, Melodelima D, N'djin WA, Souchon R, Rivoire M, Chapelon JY. Intra-operative ultrasound hand-held strain imaging for the visualization of ablations produced in the liver with a toroidal HIFU transducer: first in vivo results. Phys Med Biol. 2010; 55:3131–44. [PubMed: 20479514]

Couade M, et al. Quantitative assessment of arterial wall biomechanical properties using shear wave imaging. Ultrasound Med Biol. 2010; 36:1662–76. [PubMed: 20800942]

Damianou C, Ioannides K, Hadjisavvas V, Mylonas N, Couppis A, Iosif D, Kyriacou PA. MRI monitoring of lesions created at temperature below the boiling point and of lesions created above the boiling point using high intensity focused ultrasound. Biomedical Science and Engineering. 2010; 3:763–75.

DeWall RJ, Bharat S, Varghese T, Hanson ME, Agni RM, Kliewer MA. Characterizing the compression-dependent viscoelastic properties of human hepatic pathologies using dynamic compression testing. Phys Med Biol. 2012; 57:2273–86. [PubMed: 22459948]

Emelianov SY, Lubinski MA, Weitzel WF, Wiggins RC, Skovoroda AR, Odonnell M. Elasticity Imaging for Early Detection of Renal Pathology. Ultrasound in Medicine and Biology. 1995; 21:871–83. [PubMed: 7491743]

Fatemi M, Greenleaf JF. Ultrasound-stimulated vibro-acoustic spectrography. Science. 1998; 280:82–5. [PubMed: 9525861]

Frizzell LA, Linke CA, Carstensen EL, Fridd CW. Thresholds for Focal Ultrasonic Lesions in Rabbit Kidney, Liver, and Testicle. IEEE Trans Biomed Eng. 1977; 24:393–6. [PubMed: 881212]

Frulio H, Trillaud H. Ultrasound elastography in liver. Diagnostic and Interventional Imaging. 2013

Fry WJ, Mosberg WH, Barnard JW, Fry FJ. Production of Focal Destructive Lesions in the Central Nervous System with Ultrasound. J Neurosurg. 1954; 11:471–8. [PubMed: 13201985]

Gao Z, Lister K, Desai JP. Constitutive Modeling of Liver Tissue: Experiment and Theory. Ann Biomed Eng. 2010; 38:505. [PubMed: 19806457]

Gertner MR, Wilson BC, Sherar M. Ultrasound properties of liver tissue during heating. Ultras Med Biol. 1997; 23:1395–403.

Godfrey EM, Mannelli L, Griffin N, Lomas DJ. Magnetic Resonance Elastography in the Diagnosis of Hepatic Fibrosis. Semin Ultrasound CT MRI. 2013; 34:81–8.

Granke M, Grimal Q, Saied A, Nauleau P, Peyrin F, Laugier P. Change in porosity is the major determinant of the variation of cortical bone elasticity at the millimeter scale in aged women. Bone. 2011; 49:1020–6. [PubMed: 21855669]

Hou GY, Luo J, Marquet F, Maleke C, Vappou J, Konofagou EE. Performance Assessment of HIFU Lesion Detection by Harmonic Motion Imaging for Focused Ultrasound (HMIFU): A 3-D Finite-Element-Based Framework with Experimental Validation. Ultrasound in Med Biol. 2011; 37:2013–27. [PubMed: 22036637]

Hou GY, Marquet F, Wang S, Konofagou EE. Multi-parametric Assessment of High Intensity Focused Ultrasound (HIFU) Monitoring by Harmonic Motion Imaging for Focused Ultrasound (HMIFU): An Ex Vivo Feasibility Study. Phys Med Biol. 2013 submitted.

Huang WH, Chui CK, Kobayashi E, Teoh SH, Chang S. Multi-scale model for investigating the electrical properties and mechanical properties of liver tissue undergoing ablation. Int J CARS. 2011; 6:601–7.

Kallel F, Ophir J, Magee K, Krouskop TA. Elastographic Imaging of Low-Contrast Elastic Modulus Distributions in Tissue. Ultras Med Biol. 1998; 24:409–25.

Kallel F, Price RE, Konofagou E, Ophir J. Elastographic imaging of the normal canine prostate in vitro. Ultrason Imaging. 1999a; 21:201–15. [PubMed: 10604801]

Kallel F, Stafford RJ, Price RE, Righetti R, Ophir J, Hazle JD. The feasibility of elastographic visualization of IFU-induced thermal lesions in soft tissues. Ultras Med Biol. 1999b; 25:641–7.

Khokhlova TD, Canney MS, Khokhlova VA, Sapozhnikov OA, Crum LA, Bailey MR. Controlled tissue emulsification produced by high intensity focused ultrasound shock waves and millisecond boiling. J Acoust Soc Am. 2011; 130:3498–510. [PubMed: 22088025]

Kiss MZ, D MJ, Varghese T. Investigation of Temperature-Dependent Viscoelastic Properties of Thermal Lesions in ex vivo. Animal Liver Tissue J Biomech. 2009; 42:959–66.

Klatt D, Friedrich C, Korth Y, Vogt R, Braun J, Sack I. Viscoelastic properties of liver measured by oscillatory rheometry and multifrequency magnetic resonance elastography. Biorheology. 2010; 47:133–41. [PubMed: 20683156]

Krouskop TA, Wheeler TM, Kallel F, Garra BS, Hall T. Elastic Moduli of Breast and Prostate Tissues under Compression. Ultrasonic Imaging. 1998; 20:260–74. [PubMed: 10197347]

Kruse SA, Lawrence AJ, Dresner MA, Manduca A, Greenleaf JF, Ehman RL. Tissue characterization using magnetic resonance elastography: Preliminary results. Phys Med Biol. 2000; 45:1579–90. [PubMed: 10870712]

Li CX, Xu GL, Jiang ZY, Li JJ, Luo GY, Shan HB, Zhang R, Li Y. Analysis of clinical effect of high-intensity focused ultrasound on liver cancer. World Journal of Gastroenterology. 2004; 10:2201–4. [PubMed: 15259065]

Maleke C, Konofagou EE. Harmonic motion imaging for focused ultrasound (HMIFU): A fully integrated technique for sonication and monitoring of thermal ablation in tissues. Phys Med Biol. 2008; 53:1773–93. [PubMed: 18367802]

Maleke C, Konofagou EE. In vivo feasibility of real-time monitoring of focused ultrasound surgery (FUS) using harmonic motion imaging (HMI). IEEE Trans Biomed Eng. 2009; 57:7–11. [PubMed: 19643703]

Marra SP, Daghlian CP, Fillinger MF, Kennedy FE. Elemental composition, morphology and mechanical properties of calcified deposits obtained from abdominal aortic aneurysms. Acta Biomater. 2006; 2:515–20. [PubMed: 16839827]

McGee, H. On Food and Cooking. New York, NY: Charles Scribner's Sons; 1984.

Mueller S, Sandrin L. Liver stiffness: a novel parameter for the diagnosis of liver disease. Hepatic Medicine: Evidence and Research. 2010; 2:49–67. [PubMed: 24367208]

Muthupillai R, Lomas DJ, Rossman PJ, Greenleaf JF, Manduca A, Ehman RL. Magnetic-Resonance Elastography by Direct Visualization of Propagating Acoustic Strain Waves. Science. 1995; 269:1854–7. [PubMed: 7569924]

Nightingale KR, Palmeri ML, Nightingale RW, Trahey GE. On the feasibility of remote palpation using acoustic radiation force. J Acoust Soc Am. 2001; 110:625–34. [PubMed: 11508987]

Ophir J, Cespedes I, Ponnekanti H, Yazdi Y, Li X. Elastography: A Quantitative Method for Imaging the Elasticity of Biological Tissues. Ultras Imaging. 1991; 13:111–34.

Parker KJ, Huang SR, Musulin RA, Lerner RM. Tissue response to mechanical vibrations for sonoelasticity imaging. Ultrasound Med Biol. 1990; 16:241–6. [PubMed: 2194336]

Righetti R, Kallel F, Stafford RJ, Price RE, Krouskop TA, Hazle JD, Ophir J. Elastographic characterization of HIFU-induced lesions in canine livers. Ultras Med Biol. 1999; 25:1099–113.

Samali A, Holmberg CI, Sistonen L, Orrenius S. Thermotolerance and cell death are distinct cellular responses to stress: dependence on heat shock proteins. FEBS Lett. 1999; 461:306–10. [PubMed: 10567716]

Sandrin L, Fourquet B, Hasquenoph JM, Yon S, Fournier C, Mal F, Christidis C, Ziol M, Poulet B, Kazemi F, Beaugrand M, Palau R. Transient elastography: A new noninvasive method for assessment of hepatic fibrosis. Ultrasound in Medicine and Biology. 2003; 29:1705–13. [PubMed: 14698338]

Sapin de Brosses E, Gennisson JL, Pernot M, Fink M, Tanter M. Temperature dependence of the shear modulus of soft tissues assessed by ultrasound. Phys Med Biol. 2010; 55:1701–18. [PubMed: 20197599]

Sapin de Brosses E, Pernot M, Tanter M. The link between tissue elasticity and thermal dose in vivo. Phys Med Biol. 2011; 56:7755–65. [PubMed: 22094357]

Sarvazyan AP, Rudenko OV, Swanson SD, Fowlkes JB, Emelianov SY. Shear wave elasticity imaging: A new ultrasonic technology of medical diagnostics. Ultrasound Med Biol. 1998; 24:1419–35. [PubMed: 10385964]

Shahmirzadi D, Konofagou EE. Detection of Aortic Wall Inclusions Using Regional Pulse Wave Propagation and Velocity *In Silico*. Artery Research. 2012; 6:114–23.

Shahmirzadi D, Li RX, Konofagou EE. Pulse-Wave Propagation in Straight-Geometry Vessels for Stiffness Estimation: Theory, Simulations, Phantoms and In Vitro Findings. J Biomechanical Engineering. 2012; 134:1145021–6.

Shi XG, Martin RW, Rouseff D, Vaezy S, Crum LA. Detection of high intensity focused ultrasound liver lesions using dynamic elastometry. Ultrason Imaging. 1999; 21:107–26. [PubMed: 10485565]

Souchon R, Bouchoux G, Maciejko E, Lafon C, Cathignol D, Bertrand M, Chapelon JY. Monitoring the formation of thermal lesions with heat-induced echo-strain imaging: A feasibility study. Ultrasound in Medicine and Biology. 2005; 31:251–9. [PubMed: 15708465]

Techavipoo U, Varghese T, Zagzebski JA, Stiles T, Frank G. Temperature dependence of ultrasonic propagation speed and attenuation in canine tissue. Ultras Imaging. 2002; 24:246–60.

Ter Haar G, Clarke RL, Vaughan MG, Hill CR. Trackless surgery using focused ultrasound: Technique and case report. Minimally Invasive Therapy and Allied Technologies. 1991a; 1:13–9.

Ter Haar G, Rivens I, Chen L, Riddler S. High-Intensity Focused Ultrasound for the Treatment of Rat-Tumors. Phys Med Biol. 1991b; 36:1495–501. [PubMed: 1754620]

Thittai AK, Galaz B, Ophir J. Visualization of Hifu-Induced Lesion Boundaries by Axial-Shear Strain Elastography: A Feasibility Study. Ultrasound in Medicine and Biology. 2011; 37:426–33. [PubMed: 21276656]

Vallancien G, Harouni M, Veillon B, Mombet A, Prapotnich D, Brisset JM, Bougaran J. Focused extracorporeal pyrotherapy: Feasibility study in man. Endourology. 1992; 6:173–81.

Vappou J, Hou GY, Marquet F, Shahmirzadi D, Konofagou EE. Measuring elastic properties of biological tissues by using Focused Ultrasound-based internal indentation. UMB. 2013 under review.

Vappou J, Maleke C, Konofagou EE. Quantitative viscoelastic parameters measured by harmonic motion imaging. Phys Med Biol. 2009; 54:3579–94. [PubMed: 19454785]

Venkatesh SK, Yn M, Ehman RL. Magnetic Resonance Elastography of Liver: Technique, Analysis, and Clinical Applications. J Magnetic Resonance Imaging. 2013; 37:544–55.

Wang ST, Frenkel V, Zderic V. Optimization of pulsed focused ultrasound exposures for hyperthermia applications. J Acoustical Society of America. 2011; 130:599–609.

Wang TY, Hall TL, Xu Z, Fowlkes JB, Cain CA. Imaging Feedback of Histotripsy Treatments Using Ultrasound Shear Wave Elastography. IEEE Trans Ultrason Ferroelectr Freq Control. 2012; 59:1167–81. [PubMed: 22711412]

Warwick R, Pond J. Trackless Lesions in Nervous Tissues Produced by High Intensity Focused Ultrasound (High-Frequency Mechanical Waves). J Anat. 1968; 102:387–405. [PubMed: 4968493]

Weinberg EJ, Shahmirzadi D, Mofrad MRK. On the Multiscale Modeling of Heart Valve in Health and Disease. Biomech Model Mechano. 2010; 9:373–87.

Wiederhorn NM, Reardon GV. Studies concerned with the structure of collagen. II: stress–strain behavior of thermally contracted collagen. J Polym Sci. 1952; 9:315–25.

Wu F, Chen W, Bai J. Effect of high-intensity focused ultrasound on patients with hepatocellular cancer–preliminary report. Chinese Journal of Ultrasonog. 1999; 8:213–6.

Wu F, Wang ZB, Chen WZ, Zou JZ, Bai J, Zhu H, Li KQ, Jin CB, Xie FL, Su HB. Advanced hepatocellular carcinoma: Treatment with highintensity focused ultrasound ablation combined with transcatheter arterial embolization. Radiology. 2005a; 235:659–67. [PubMed: 15858105]

Wu F, Wang ZB, Zhu H, Chen WZ, Zou JZ, Bai J, Li KQ, Jin CB, Xie FL, Su HB. Extracorporeal high intensity focused ultrasound treatment for patients with breast cancer. Breast Cancer Research and Treatment. 2005b; 92:51–60. [PubMed: 15980991]

Wu T, Felmlee JP, Greenleaf JF, Riederer SJ, Ehman RL. Assessment of thermal tissue ablation with MR elastography. Magn Reson Med. 2001; 45:80–7. [PubMed: 11146489]

Xu Z, Hall T, Fowlkes J, Cain C. Effects of acoustic parameters on bubble cloud dynamics in ultrasound tissue erosion (histotripsy). J Acoust Soc Am. 2007; 122:229–36. [PubMed: 17614482]

Zhang M, Nigwekar P, Castaneda B, Hoyt K, Joseph JV, Di Sant'Agness A, Messing EM, Strang JG, Rubens DJ, Parker KJ. Quantitative Characterization of Viscoelastic Properties of Human Prostate Correlated with Histology. Ultras Med Biol. 2008; 34:1033–42.

Zhou Y. Generation of uniform lesions in high intensity focused ultrasound ablation. Ultrasonics. 2013; 53:495–505. [PubMed: 23106859]

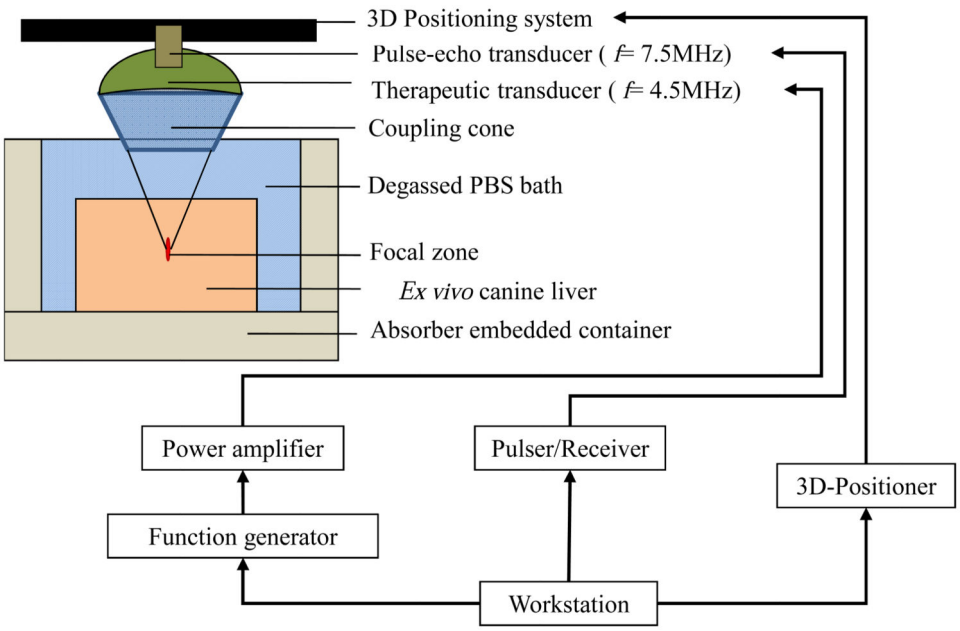

Figure 1.

Schematics of High Intensity Focused Ultrasound (HIFU) experimental set up used to induce conglomerate set of thermally-ablated lesions; Adapted (Hou et al. 2011). The pulse-echo and therapeutic transducers were used for targeting (no image acquisition) during raster scan and ablation, respectively.

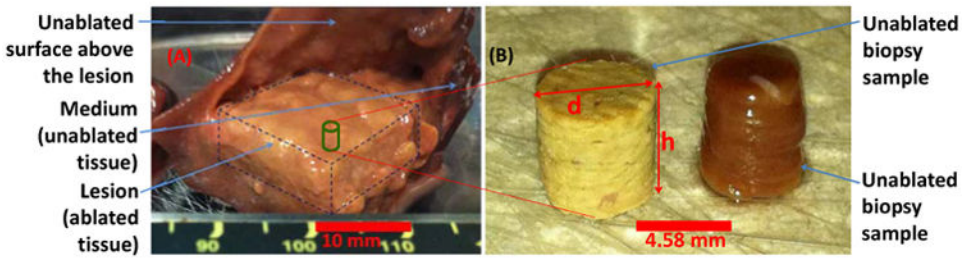

Figure 2.

(A) Image of a 15×15 mm^2 inclusion composed of a group of thermally-ablated lesions obtained by raster HIFU ablation on canine liver tissue *ex vivo*, (B) Representative biopsy samples from unablated and ablated canine liver tissues.

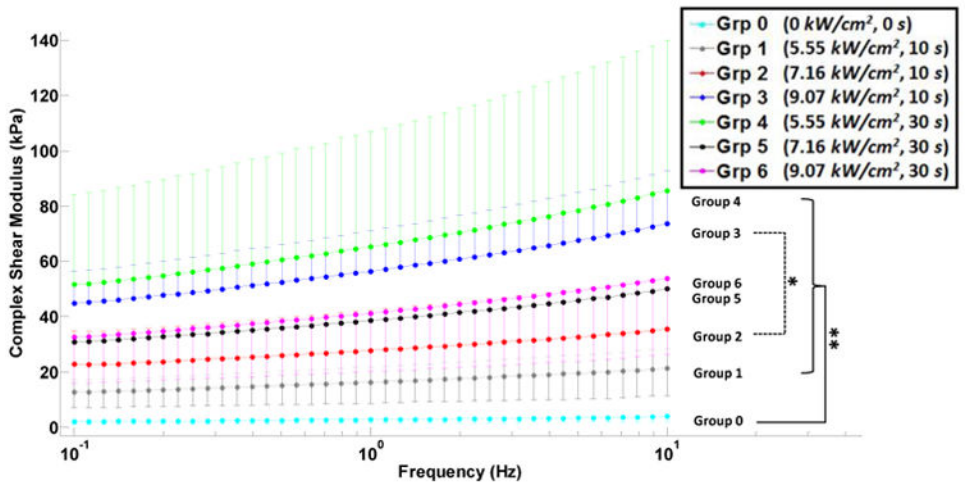

Figure 3.

Complex shear modulus versus applied shear strain frequency (semi-log scale) for unablated, group 0, and ablated, groups 1-6, canine liver tissue samples. The error bars (either upward or downward) indicate the standard deviations of multiple measurements on different samples. Inter-group significant difference is indicated with * ($p<0.05$) and ** ($p<0.001$).

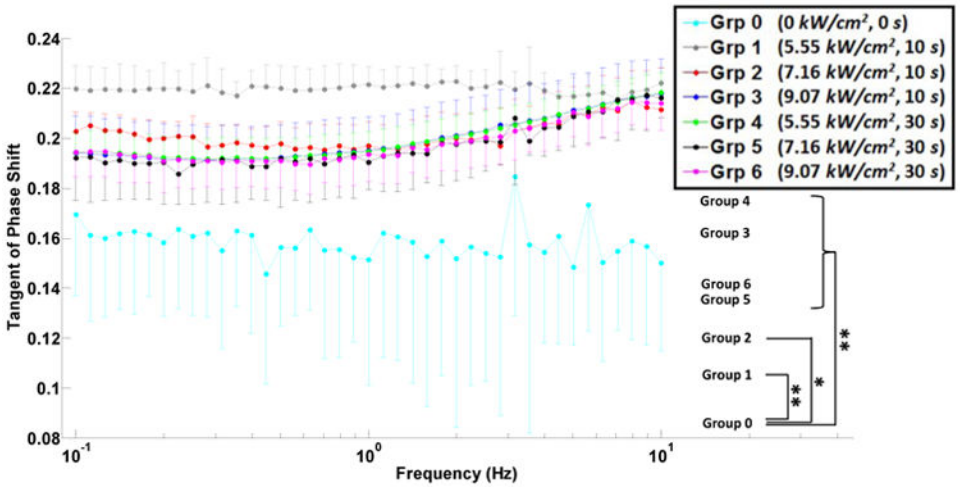

Figure 4.

Tangent of the stress-strain phase shift versus applied shear strain frequency (semi-log scale) for unablated, group 0, and ablated, groups 1-6, canine liver tissue samples. The error bars (either upward or downward) indicate the standard deviations of multiple measurements on different samples. Inter-group significant difference is indicated with * ($p<0.05$) and ** ($p<0.001$).

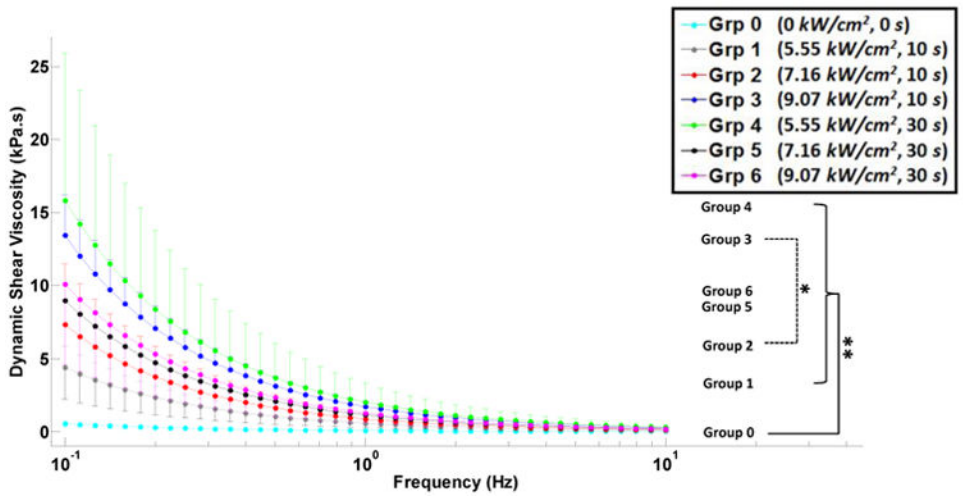

Figure 5.

Dynamic shear viscosity versus applied shear strain frequency (semi-log scale) for unablated, group 0, and ablated, groups 1-6, canine liver tissue samples. The error bars (either upward or downward) indicate the standard deviations of multiple measurements on different samples. Inter-group significant difference is indicated with * ($p<0.05$) and ** ($p<0.001$).

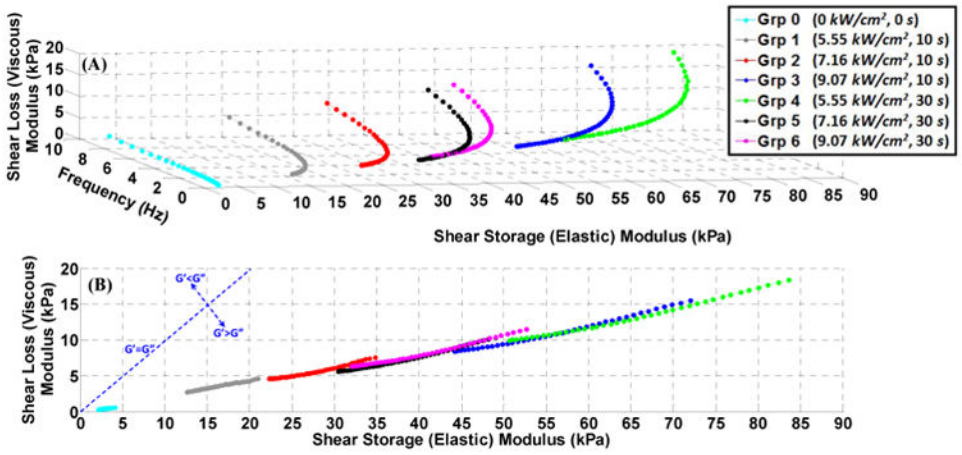

Figure 6.

The storage (elastic) modulus against the loss (viscous) modulus for unablated, group 0, and ablated, groups 1-6, samples: (A)3D plot with the frequency on the azimuth axis, (B)2D projection on the loss-storage plane marking the border line of the equal elasticity-viscosity contributions. The upper-left of the line indicates the viscous-dominant zone, and the lower-right of the line, where all the unablated and ablated tissues are located, indicates the elastic-dominant zone.

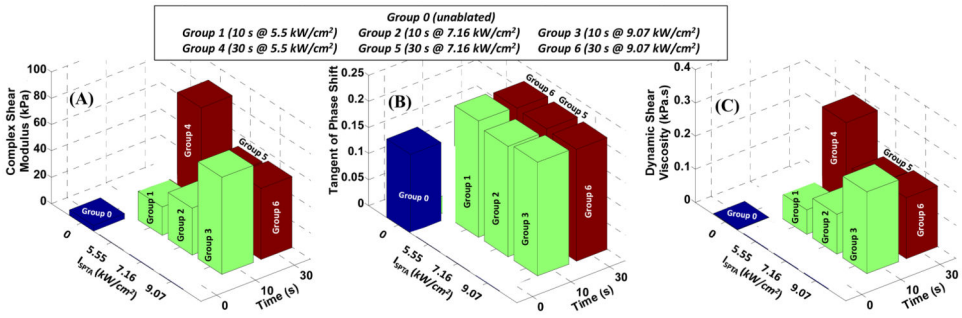

Figure 7.

The contrast plot indicating the relative change in each of the tissue viscoelastic parameters versus HIFU *in situ* power and time: (A)shear complex, (B)tangent of the phase shift, (C)shear viscosity coefficient.

Table 1

Experimental HIFU intensity and time period for ablated groups 1-6 are provided. A set of unablated samples was maintained as the control group, group 0.

Group Number	*In situ* I_{SPTA} (kW/cm^2)	*In situ* Acoustic Power (W)	Time Duration (s)
0	0	0	0
1	5.55	8	10
2	7.16	10	10
3	9.07	11	10
4	5.55	8	30
5	7.16	10	30
6	9.07	11	30

Table 2

The change in viscoelastic properties of ablated tissues, groups 1-6, normalized by those of the unablated tissues. The average and standard deviation values are obtained over the entire frequency range of 0.1-10 *Hz*.

	Group 1 **10 *s* @ 5.55 *kW/cm²***	**Group 2** **10 *s* @ 7.16 *kW/cm²***	**Group 3** **10 *s* @ 9.07 *kW/cm²***	**Group 4** **30 *s* @ 5.55 *kW/cm²***	**Group 5** **30 *s* @ 7.16 *kW/cm²***	**Group 6** **30 *s* @ 9.07 *kW/cm²***
Normalized shear complex modulus	5.77±0.13	9.83±0.36	19.98±0.52	23.09±0.53	13.66±0.39	14.06±0.36
Normalized tangent of the phase shift	1.390±0.060	1.274±0.064	1.262±0.082	1.263±0.081	1.264±0.08	1.251±0.077
Normalized shear viscosity coefficient	8.19±0.26	12.98±0.45	25.49±0.97	30.14±1.15	16.95±0.63	19.02±0.68